JACS
JOURNAL OF THE AMERICAN CHEMICAL SOCIETY

Article

pubs.acs.org/JACS

Surprisingly High Selectivity and High Affinity in Mercury Recognition by H-Bonded Cavity-Containing Aromatic Foldarands

Jie Shen,[†] Changliang Ren,[†] and Huaqiang Zeng*[,†]

[†]Institute of Bioengineering and Nanotechnology, 31 Biopolis Way, The Nanos, Singapore 138669

Supporting Information

ABSTRACT: In the absence of macrocyclic ring constraints, few synthetic systems, possessing a mostly solvent-independent well-folded conformation that is predisposed for highly selective and high affinity recognition of metal ions, have been demonstrated. We report here such a unique class of conformationally robust modularly tunable folding molecules termed foldarands that can recognize Hg^{2+} ions surprisingly well over 22 other metal ions. Despite the lack of sulfur atoms and having only oxygen-donor atoms in its structure, the best foldarand molecule, i.e., tetramer **4**, exhibits a selectivity factor of at least 19 in differentiating the most tightly bound Hg^{2+} ion from all other metal ions, and a binding capacity that is ≥18 times that of thio-crown ethers. These two noteworthy binding characters make possible low level removal of Hg^{2+} ions. With a [**4**]:[Hg^{2+}] molar ratio of 5:1 and a single biphasic solvent extraction, the concentration of Hg^{2+} ions could be reduced drastically by 98% (from 200 to 4 ppb) in pure water. **4** could also effect a highly efficient reduction in mercury content by 98% (from 500 to 10 ppb) in artificial groundwater via multiple successive extractions with an overall consumption of **4** being 9:1 in terms of [**4**]:[Hg^{2+}] molar ratio.

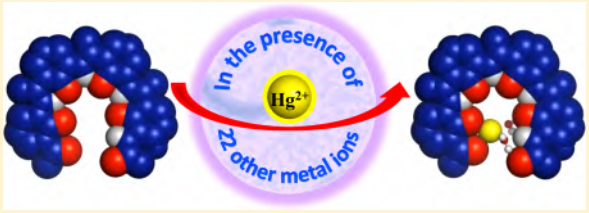

INTRODUCTION

The ability of naturally occurring biomolecules such as proteins and DNAs to fold into well-defined three-dimensional structures has inspired many scientists to research actively synthetic abiotic foldamers[1a] that are similarly capable of adopting stable, compact conformations in an effort to not only imitate the natural biopolymers in structure but also eventually rival them in function or create new functions unseen in Nature.[1] The conformational folding of these foldamer molecules is generally realized through the use of noncovalent forces including H-bonds, solvophobic interactions, $\pi-\pi$ stacking and metal coordination bonds. Such a folding often generates diverse sizable cavities decorated by appropriate functional groups, from which highly variable functions have been demonstrated. Notable examples include recognition of neutral (saccharides,[2a−c] water[2d−h] and other small molecules[2i−p]) or ionic[3,4] species as well as biologicals,[5a,b] solvent gelation,[5c−e] liquid-crystalline materials,[5f] reaction catalysis,[5g−j] reactive sieving,[5i,k−n] ion/water transport across the cell membranes[5o−t] and electron/hole transfer.[5u]

A prime strategy for recognizing inorganic cationic species in the contemporary foldamer research involves designing adaptive abiotic foldamers that frequently take a helical structure and generally undergo a dramatic folding/unfolding process in response to ions or solvent polarity. These include helicates,[3a−f] phenylacetylene-based oligomers,[3g] bilinone derivatives,[3h] metallofoldamers,[4b,c] oligocholates[4d,5q] and oxime peptides.[4i] Tactics for constructing acyclic folding molecules, having a 2D-shaped or helically folded conformation that is robust and insensitive toward solvent polarity and ion binding but yet properly predisposed for highly selective high-affinity recognition of metal ions, have remained largely unexplored.

In analogy to diverse ion-binding ligands such as corands by Pedersen,[6a,b] cryptands by Lehn,[6c,d] spherands by Cram[6e,f] and torands by Bell,[6g,h] we describe here a novel class of acyclic modularly tunable cation-binding foldamer molecules termed foldarands. In the absence of macrocyclic ring constraints, these acyclic pyridone-based foldarands still possess a mostly solvent-independent H-bond-rigidified robust conformation, which is resilient toward both nonpolar and polar solvents including water[7] and exhibits insignificant conformational changes even upon ion-binding. In connection with this definition, a few precedents arguably do exist in the literature as reported by Ueyama,[8a] Gong,[8b] Li[3i,8c] and our group.[8d,e] Nevertheless, these H-bonded aromatic foldamer molecules have not proven useful for consistent and highly selective high-affinity recognition of metal ions. Various reasons to account for their inherent inability in ion recognition include (1) molecular instability,[8a] (2) oversized cavity of >3.8 Å in radius after excluding the van der Waals volume of ion-binding atoms,[8b] (3) presence of inward-pointing hydrophobic alky groups that block the cavity of otherwise suitable size for ion binding[8c−e] and (4) the donor atoms' intrinsic poor binding affinity toward metal ions.[3i]

The specific pyridone-based acyclic foldarands **1**−**6** studied in our current investigation are characterized (1) by having multiple neutral electron-rich donor atoms whose inward-pointing convergent alignment for ion binding is attained via noncovalent intramolecular H-bonds, rather than covalent

Received: January 4, 2017
Published: February 2, 2017

DOI: 10.1021/jacs.6b13342
J. Am. Chem. Soc. 2017, 139, 5387−5396

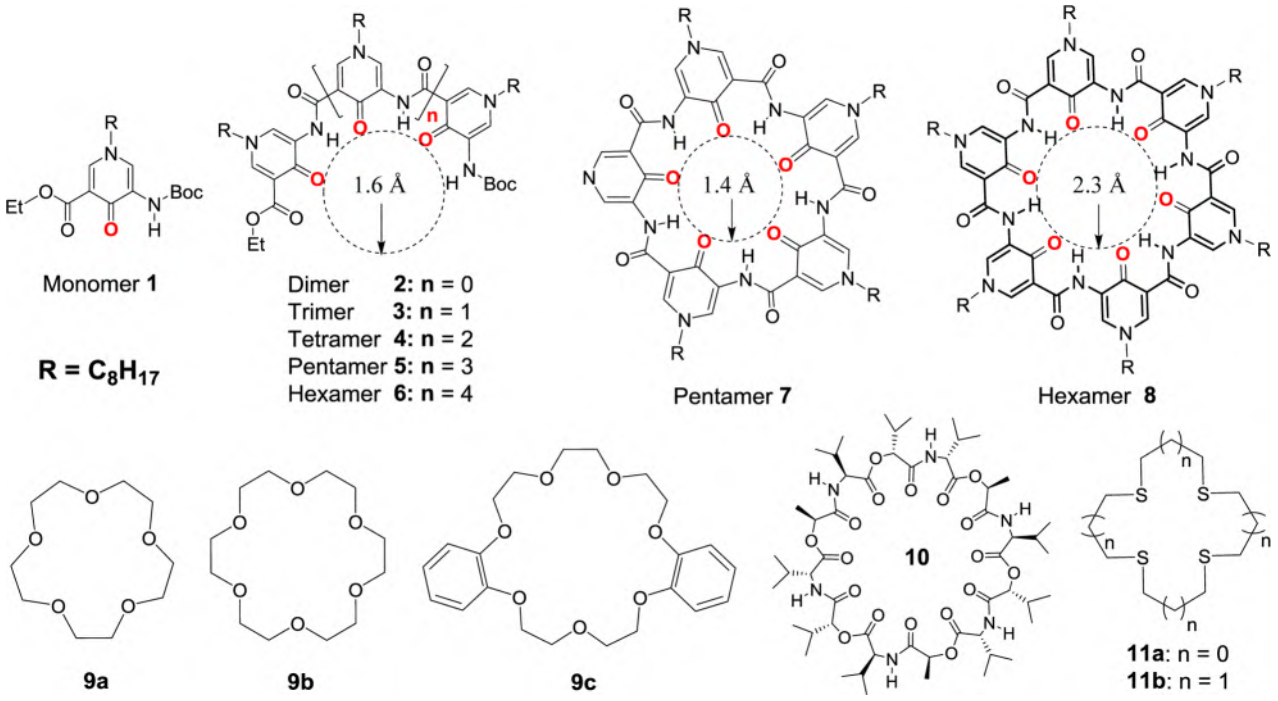

forces as seen in the macrocyclic precedents and (2) further by having minimum conformational changes resulting from ion coordination and binding, a property akin to those seen in macrocyclic cryptands,[6c,d] spherands[6e,f] and torands.[6g,h] This rigidity in backbone also may aid to enhance the binding specificity. These foldarands additionally feature proper separation involving multiple oxygen-donor atoms enforced by the H-bonding-rigidified crescent-shaped backbone, creating a noncollapsible cavity of ~1.6 Å in radius (or ~3.1 Å from the cavity center to the nucleus of the interior O atoms) suitable for hosting a partially hydrated metal ion to achieve selective recognition of metal ions.

In this article, we have thoroughly and systematically investigated the ion-differentiating ability of **1**–**6** and their other variants toward 23 metal ions using a binary water–$CHCl_3$ extraction system, and report here their unexpectedly high selectivity and high affinity in recognizing and extracting Hg^{2+} ions with respect to the other 22 metal ions. These surprising findings are in sharp contrast with the ion-binding profiles of their cyclic analogues, pentamer **7** and hexamer **8**, exhibiting weak or no binding of Hg^{2+} ions but predominant recognition of Cs^{+}[4j] and Cu^{2+},[4l] respectively, in the presence of many other metal ions. These findings further demonstrate surprisingly consistent and superior performance for Hg^{2+} recognition by foldarands **1**–**6** compared to various O- or S-containing macrocycles **9**–**11** and kryptonfix-222,[4k] given that Hg^{2+} ions prefer soft S atom over hard O atom. Aside from a unique ability in recognizing Hg^{2+} ions, **1**–**4** are also capable of binding other ions including K^{+}, Ca^{2+} and Ag^{+} to various degrees, with **5** and **6** preferring Cs^{+}, Ba^{2+} and Pb^{2+} ions over Rb^{+}, K^{+}, Na^{+}, Ag^{+}, Ca^{2+} and Cu^{2+} ions.

RESULTS AND DISCUSSION

Computational Elucidation and Crystallographic Verification of Foldarands' Folded Structures. First principle calculation at the B3LYP/6-31G(d,p) level has proven to be highly reliable in consistently and accurately predicting the H-bond-rigidified structures of diverse folding molecules, which were verified later by their crystal structures.[9] Hence, calculations using chloroform as the explicit solvent were performed to estimate the cavity size enclosed in acyclic foldarands **1**–**6**. The computationally determined structures show that, with increasing addition of pyridone-based building blocks, the progressively lengthened backbone becomes increasingly curved in one direction and eventually adopts a helically folded structure (Figure 1a–f). These crescent-shaped structures are induced by strongly stabilizing forces from the H-bonding network comprising up to 11 intramolecular H-bonds (NH···O═C, 1.81–2.30 Å). The end-to-end steric repulsion makes **4** deviate from planarity seen in **1**–**3**, and further works with strong repulsion between the end O atoms to produce a well-defined helical structure in **5** and **6**. Starting from **3**, an enclosed cavity of about 1.6 Å in radius exclusive of van der Waals volume of O atoms becomes visible in **3**–**6** with their interiors decorated by three to six pyridone O atoms.

The computationally derived crescent-shaped structures adopted by foldarands **2**–**6** can be verified experimentally through the crystallographic study of trimer **12** with single crystals obtained by slow diffusion of 1.2 mL of EtOH into 0.5 mL of **12**-containing DMSO at room temperature for about 1 month). In the solid state (Figure 1g), **12** folds into a nearly planar curved conformation that is remarkably similar to the optimized structure of **3** at the B3LYP/6-31G(d,p) level (Figure 1c). A continuous H-bonding network made up of five intramolecular H-bonds (5- and 6-membered NH···O═C = 2.192–2.330 and 1.850–1.927 Å, respectively) brings three pyridone O atoms in a crescent manner to enclose a small cavity of ~1.6 Å in radius, near-identical to that of the computationally determined cavity in **3**. This comparative structural study demonstrates reliability and high applicability of first principle computation at the B3LYP/6-31G(d,p) level in obtaining accurate structural representations for H-bonded aromatic foldamers including foldarands **1**–**6**.

Highly Selective and High-Affinity Recognition of Hg^{2+} Ions by Foldarands. The pyridone unit used to construct **1**–**6** has an aromatic resonance structure in which its

DOI: 10.1021/jacs.6b13342
J. Am. Chem. Soc. 2017, 139, 5387–5396

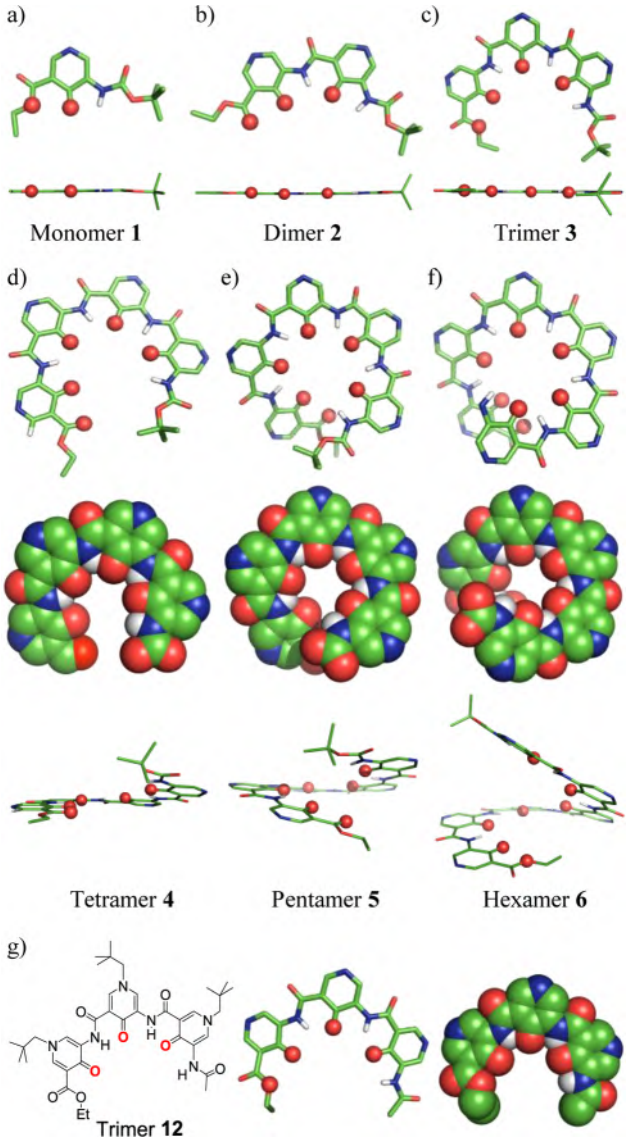

Figure 1. (a–f) Top and side views of computationally optimized structures for foldarands **1**–**6** at the B3LYP/6-31G(d,p) level using chloroform as the explicit solvent. (g) Crystal structure of trimer **12**. In the images, all interior O atoms that might be involved in binding metal cations are highlighted as red balls with all side chains, aromatic H atoms and H atoms of ethyl and Boc groups removed for clarity of view. Repulsions between the end groups and among pyridone O atoms lead to unusually large helical pitches in **5** and **6**. From the CPK representations built on the basis of van der Waals radius (Gray, H = 1.20 Å; Green, C = 1.70 Å; Blue, N = 1.55 Å; Red, O = 1.52 Å), a cavity size of ~1.6 Å in radius formed by three to six carbonyl O atoms is clearly visible in foldarands **4**–**6** and **12**.

N atom is positively charged and acts as an electron donor with carbonyl O atom at para position carrying a negative charge and serving as an electron acceptor. This push–pull effect results in a much higher yet donarable electron density, residing at pyridone O atom, than that around conventional carbonyl O atoms. This provides foldarands **1**–**6** with higher ability to strip off water molecules from the hydrated metal ions. Further considering that majority of metal cations possess a radius of <1.6 Å, a cavity of ~1.6 Å in radius contained in **3**–**6** therefore might suggest efficient yet differential interactions between **3**–**6** and cations of varying sizes.

To validate the hypothesis underlying the use of foldarands **1**–**6** for selective recognition and extraction of metal ions, we carried out biphasic extraction experiments using equal volumes of H_2O containing 18 metal ions in their nitrate salts, each at 0.1 mM, and $CHCl_3$ containing an organic host (e.g., **1**–**8**, crown ethers **9**, valinomycin **10** and thio-crown ethers **11**) at 0.12 mM at 25 °C (Figure 2). Ion extractions from aqueous phase to chloroform layer were followed by measuring the residual concentrations of various metal ions in H_2O layer using inductively coupled plasma mass spectrometry (ICP-MS). Data compiled in Figure 2 reveal a very surprising yet persistent binding behavior by **1**–**6**, particularly in comparison with structurally similar ligands **7** and **8** and with those O- or S-containing macrocycles **9**–**11**. On one hand, while macrocyclic hosts **7**[4j] and **8**[4l] preferentially bind Cs^+ and Cu^{2+} ions, respectively, foldarands **1**–**6** invariably exhibit the strongest binding toward Hg^{2+} ions with extraction efficiencies ranging from 12 to 54% in the presence of 17 other metal ions at a [host]:[Hg^{2+}] molar ratio of 1.2:1. Moreover, extractions of these 17 metal ions by **1**–**6** remain at the undetectable levels within the instrument's capacity. On the other hand, the best extraction efficiency by **9**–**11** is 11% of K^+ ions by **9b** with macrocyclic ligands **9c**, **10** and **11a** incapable of extracting any of 18 metal ions from aqueous to chloroform phase. Notably, S-containing soft ligands **11** can hardly extract Hg^{2+} ions out of aqueous solution under the identical conditions. These data demonstrate the capacity of ligands to extract their respective most extractable metal ions to increase in the order of **9c** ≅ **10** ≅ **11a** < **11b** < **9a** ≅ **9b** < **1** < **2** < **7** < **3** < **5** ≅ **6** < **4**, a relative trend that might also reflect a relative order of the ligands' binding affinity toward the respective metal ions. Such a difference in ion-binding affinity between pyridone-based hosts **1**–**8** and the more flexible hosts (crown ethers, valinomycin and thio-crowns) likely can be attributed to the H-bonded rigid backbone in **1**–**8** that produces a convergent alignment of O atoms whose electron density is significantly higher than that of the O atoms found in **9** and **10**, and possibly even higher than that of S atoms in **11**.

Additional testing of 5 more metal ions (e.g., Co^{2+} and Cr^{3+} in their nitrate salts and Au^+, Pt^{2+} and Pd^{2+} in their chloride salts) similarly reveals no detectable extraction of these metal ions by **1**–**6**, suggesting a low likelihood for these 5 metal ions to strongly compete with Hg^{2+} ions in binding to **1**–**6**. Indeed, compared to the extraction efficiencies obtained in the presence of 17 other metal ions, the extraction efficiency of Hg^{2+} ions (0.1 mM) in the absence of 17 metal ions using **1**–**6** at 0.12 mM increases only marginally by 6–11% to 18, 28, 48, 64, 62 and 61%, respectively, confirming a highly selective nature of **1**–**6** in binding and extracting Hg^{2+} ions.

To obtain comprehensive binding and extraction profiles of **1**–**6** toward metal ions of varying types, similar biphasic extraction experiments were performed at 25 °C with an increasing concentration of host from 0.12 mM to 0.54, 0.90 and 1.80 mM with 18 metal ions each fixed at 0.10 mM (Table S1).

With an increase in concentration of hosts **1**–**6** from 0.12 to 0.54 mM, extraction efficiencies for Hg^{2+} dramatically increase from 12, 19 and 39% to 45, 52 and 78% for **1**–**3**, respectively, whereas efficient extractions of 81–92% Hg^{2+} were observed for **4**–**6**. Moreover, ligand-mediated extraction of Hg^{2+} by **1**–**6** appears to be highly selective with **4** as the best in terms of both affinity and selectivity toward Hg^{2+} ions. For **1** and **2** at 0.54 mM and assuming formation of 2:1 ligand:Hg^{2+} ion complexes,

DOI: 10.1021/jacs.6b13342
J. Am. Chem. Soc. 2017, 139, 5387–5396

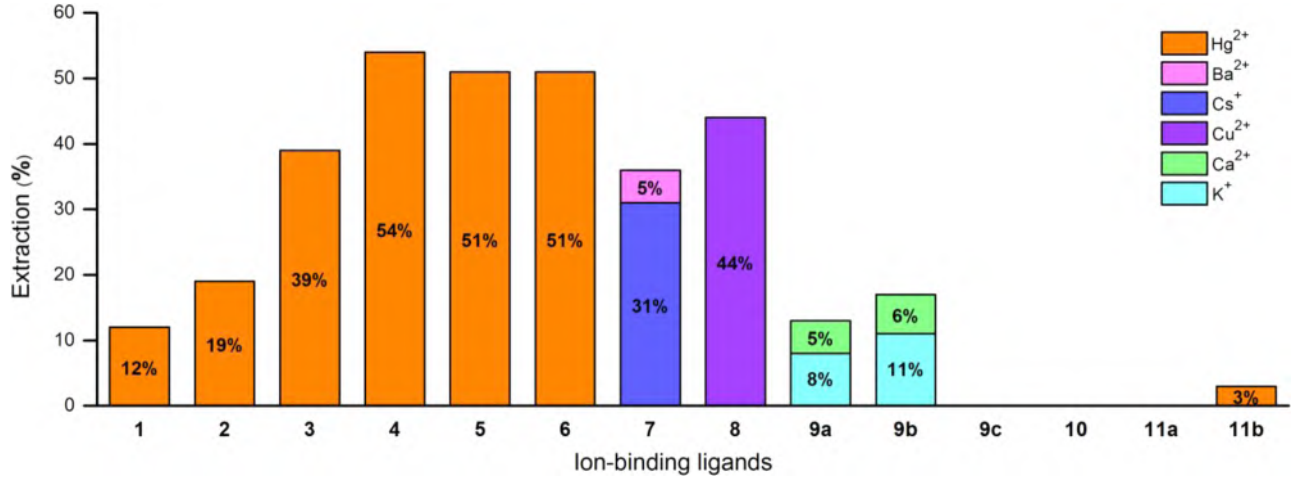

Figure 2. Extractable ions (%) and extraction capacity by acyclic foldarands **1**−**6** and macrocyclic hosts **7**−**11** determined using ICP-MS. Extractions were carried out in a biphasic solvent extraction system using equal volumes of H_2O containing 18 metal ions each at 0.1 mM and $CHCl_3$ containing organic host at 0.12 mM at 25 °C. These 18 metal ions in their nitrate salts are Hg^{2+}, Li^{+}, Na^{+}, K^{+}, Rb^{+}, Cs^{+}, Mg^{2+}, Ca^{2+}, Ba^{2+}, Al^{3+}, Mn^{2+}, Fe^{3+}, Ni^{2+}, Cu^{2+}, Zn^{2+}, Ag^{+}, Cd^{2+} and Pb^{2+}. All reported data are the values that were averaged over six runs with relative errors within 3%. No detectable extraction of any metal ion by macrocyclic ligands **9c**, **10** and **11a** at 0.12 mM could be observed.

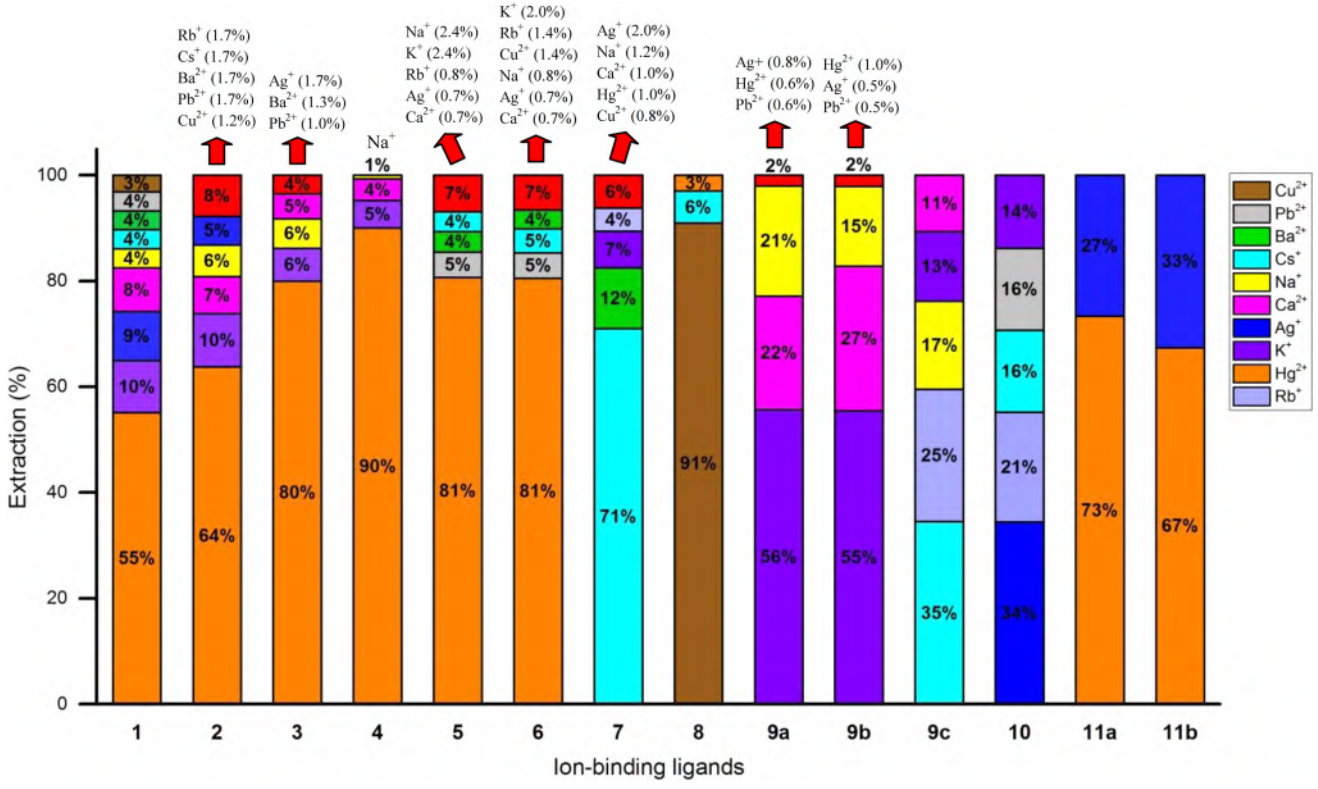

Figure 3. Schematic illustrations of ion-binding selectivities by acyclic foldarands **1**−**6** and macrocyclic hosts **7**−**11**. These relative extraction percentages, totaling 100%, are normalized on the basis of data summarized in Table S1. A red rectangular area on the top of some columns refers to the total extraction of some least extractable metal ions whose composition and extraction percentage are highlighted above the corresponding columns. For **4**, the six metal ions (Rb^{+}, Cs^{+}, Ba^{2+}, Cu^{2+}, Ag^{+} and Pb^{2+}) with a relative extraction percentage less than 0.1% were removed from the chart.

the residual concentration of unbound **1** or **2** in their Hg^{2+}-free form should be larger than 0.44 mM, which is at least 4.4-fold as much as that of any other single metal ion with an initial concentration of 0.1 mM. Nevertheless, such excessively unbound **1** or **2** is only able to extract marginally 8−18% of K^{+}, Ca^{2+} and Ag^{+} ions with no noticeable extraction of the remaining 14 metal ions. For **3** and **4** that form a 1:1 complex with Hg^{2+} and so should be present in solution with a residual concentration greater than 0.45 mM, the excessive amounts of unbound **3** and **4** also weakly bind and insignificantly extract Na^{+}, K^{+} and Ca^{2+} by 15−27%. Similarly, **5** and **6** exhibit a total extraction capacity of 289 and 326% toward 9 out of 18 metal ions, respectively, thereby leaving ∼0.25 mM of **5** and ∼0.21 mM of **6** in their uncomplexed form. Under identical

DOI: 10.1021/jacs.6b13342
J. Am. Chem. Soc. 2017, 139, 5387−5396

conditions, **7**-mediated extractions of Cs^+ and Ba^{2+} increase from 31 and 5% (Figure 2) to 97 and 90% (Table S1), respectively, whereas **8** predominantly extracts Cu^{2+} ions by 84% with the second most extractable Cs^+ ions extracted only by 8%. Upon increasing the host concentration from 0.12 mM to 0.54 mM, (1) the ability of K^+-selective crown ethers **9a** and **9b** to extract K^+ ions increases dramatically from 8 and 11% (Figure 2) to 62 and 61% (Table S1), respectively, (2) metal ions of various types still remain poorly extracted by **9c**, **10**, **11a** and **11b**, and (3) **11a** and **11b** are Hg^{2+}-selective.

The comparative trend where **1**−**6** display high-affinity and highly selective extraction of Hg^{2+} ions persists with concentrations of **1**−**6** increasing from 0.54 mM to 0.90 and 1.80 mM. Extraction of >80% Hg^{2+} was achieved consistently by using either 0.9 mM or 1.80 mM of **1**−**6**. Based on total extraction efficiency at 0.9 mM, the uncomplexed form of **1**−**6** likely exists in solution with a residual concentration of 0.65, 0.64, 0.69, 0.71, 0.36 and 0.27 mM, respectively. These correspond to at least 6.5, 6.4, 6.9, 7.1, 3.6 and 2.7 times the concentration of any single metal ion in solution. At 1.80 mM, the residual concentration of excess uncomplexed **1**−**6** further increases to 1.42, 1.40, 1.41, 1.43, 0.99 and 0.89 mM, respectively. The presence of these excessive amounts of uncomplexed ligands not only suggests ligand's weak capacity of binding many other non-Hg^{2+} ions but also confirms that their recognition of Hg^{2+} ions proceeds in a highly selective fashion with **4** being the most selective. At 1.80 mM, near-complete removals of Ba^{2+} and Pb^{2+} by **5**, and Cs^+, Ba^{2+} and Pb^{2+} by **6** were also observed.

Further analyses of extraction data and patterns on non-Hg^{2+} ions at host concentrations of 0.54, 0.90 and 1.80 mM reveal additional differentiating abilities of both foldarands **1**−**6** and macrocyclic ligands **7**−**11** in binding and extracting metal ions. As seen from the normalized relative extractions in Figure 3, ions (e.g., Na^+, K^+, Ca^{2+} and Ag^+ that are extractable by ≥5%) preferred by **1**−**4** are not preferred by **5** and **6**, and vice versa. In sharp contrast to planar **1**−**3** and helically folded **5** and **6** that are capable of recognizing 7−10 metal ions, tetramer **4** with a slightly twisted structure (Figure 1) turns out to possess the highest selectivity in Hg^{2+} recognition. At the host concentration of 1.8 mM, **4** extracts only four types of metal ions to significant extents with the relative extraction percentage of all other ions staying below 0.1% (Figure 3). It would be worth pointing out that the second most extractable ions for the ligands studied vary significantly with K^+ for **1**−**4**, Pb^{2+} for **5** and **6**, Ba^{2+} for Cs^+-selective **7**, Cs^+ for Cu^{2+}-selective **8**, Ca^{2+} for K^+-selective **9a** and **9b**, Rb^+ for Cs^+-selective **9c** and Ag^+-selective **10**, and Ag^+ for Hg^{2+}-selective **11**. Peculiarly, 15-crown-5 (**9a**), which is known to be Na^+-selective, becomes K^+-selective under the biphasic extraction conditions with a K^+/Na^+ selectivity of at least 2.7 and a pattern resembling that of 18-crown-6 (**9b**). Likewise, valinomycin (**10**), which serves as the K^+ transporter, does not favorably bind K^+ ions either (14%), and its most favored ions actually are Ag^+ (34%) and Rb^+ (21%). With respect to all other ligands studied here, it can be concluded that acyclic tetramer **4** and macrocyclic hexamer **8** display the best ion-binding profile in terms of selectivity and affinity toward their respective most extractable ions.

Low-Level Mercury Removal by 4. The above extraction experiments were all carried out with each metal ion set at 0.1 mM, which corresponds to 20 ppm in the case of Hg^{2+} ions. Because the ligands' ability to efficiently remove metal ions at high concentrations does not warrant similar ion-removing efficiencies at environmentally relevant low concentrations, we decided to also look into effectiveness of foldarands **1**−**6** in trace-level mercury removal. This is particularly important given that the permitted discharge limit for mercury set by the U.S. Environmental Protection Agency (EPA) is 10 ppb in wastewater and 2 ppb in drinking water.[10]

We first carried out the extractions using 2.5 μM (500 ppb) Hg^{2+}, a 40-fold reduction from 20 ppm. At a [host]:[Hg^{2+}] molar ratio of 1:1 (Table 1), **1**−**6** all display comparable Hg^{2+}-

Table 1. Extraction Efficiencies (%) of Hg^{2+} Ions at 2.5 μM (500 ppb) by Foldarands 1−6 As Determined by Inductively Coupled Plasma Mass Spectrometry (ICP-MS)[a]

	host:Hg^{2+} molar ratio			
host	1:1	2:1	3:1	4:1
1	20	31	43	56
2	28	40	53	69
3	49	80	92	96
4	64	92	96	99
5	66	90	95	98
6	62	86	96	98

[a]Extractions were carried out in a biphasic system using equal volumes of H_2O containing Hg^{2+} ions at 2.5 μM and $CHCl_3$ containing host from 2.5 to 10 μM at 25 °C. All reported data are averaged values over six runs with relative errors within 1%.

extraction efficiencies of 20−66% when respectively compared to those obtained at 20 ppm of Hg^{2+}. Among **1**−**6**, tetramer **4** consistently exhibits the highest extraction efficiency of 92−99% when the [host]:[Hg^{2+}] molar ratio varies from 2:1 to 4:1. In light of its synthetic ease with respect to **5** and **6**, **4** was chosen for further investigation. For the solutions containing Hg^{2+} ions at the 200, 50 and 20 ppb level and using a constant [**4**]:[Hg^{2+}] molar ratio of 5:1, our results show that **4** is able to remove Hg^{2+} ions with good efficiencies of 98, 84 and 75%, respectively. Nevertheless, **4** lacks significant ability to remove trace amounts of Hg^{2+} ions, and for the solution containing Hg^{2+} ions at 5 ppb, it could only remove 39% Hg^{2+} ions at a [host]:[Hg^{2+}] molar ratio of 500. On the basis of these extraction data, our calculations show that the amount of **4** needed to lower down Hg^{2+} ions from 5 to 3 ppb is roughly the same amount needed to decrease Hg^{2+} ions from 1000 to 5 ppb. That is, it would be more beneficial to lower the residual concentration of Hg^{2+} ions in pure water to below 5, rather than 3 ppb; otherwise, a huge amount of **4** would have to be used.

The findings on **4** in terms of high selectivity and high extraction capacity are not only interesting but also significant in view of the facts that small molecule ligands exhibiting high-affinity binding of Hg^{2+} ions are mostly derived from sulfur-containing compounds with strong odor[11a,b] and that, among many approaches developed, methods for remediating low ppb levels of Hg^{2+} are still scarce.[11c−f] Undesirably as evidenced from Table S1, K^+, Ca^{2+} and Na^+ ions commonly found in drinking and groundwater constitute the major competing cations for Hg^{2+} binding by **4**. Therefore, to exam how the abundant presence of these ions in solution might interfere with **4**-mediated removal of Hg^{2+} in the practical application, we prepared an artificial groundwater at pH 7.4 that contains 100 ppm of Na^+ (4.35 mM), 10 ppm K^+ (0.256 mM), 60 ppm of Ca^{2+} (1.50 mM), 25 ppm Mg^{2+} (1.04 mM) and 340 ppm of Cl^- (9.686 mM). This artificial groundwater is then "spiked"

DOI: 10.1021/jacs.6b13342
J. Am. Chem. Soc. 2017, 139, 5387−5396

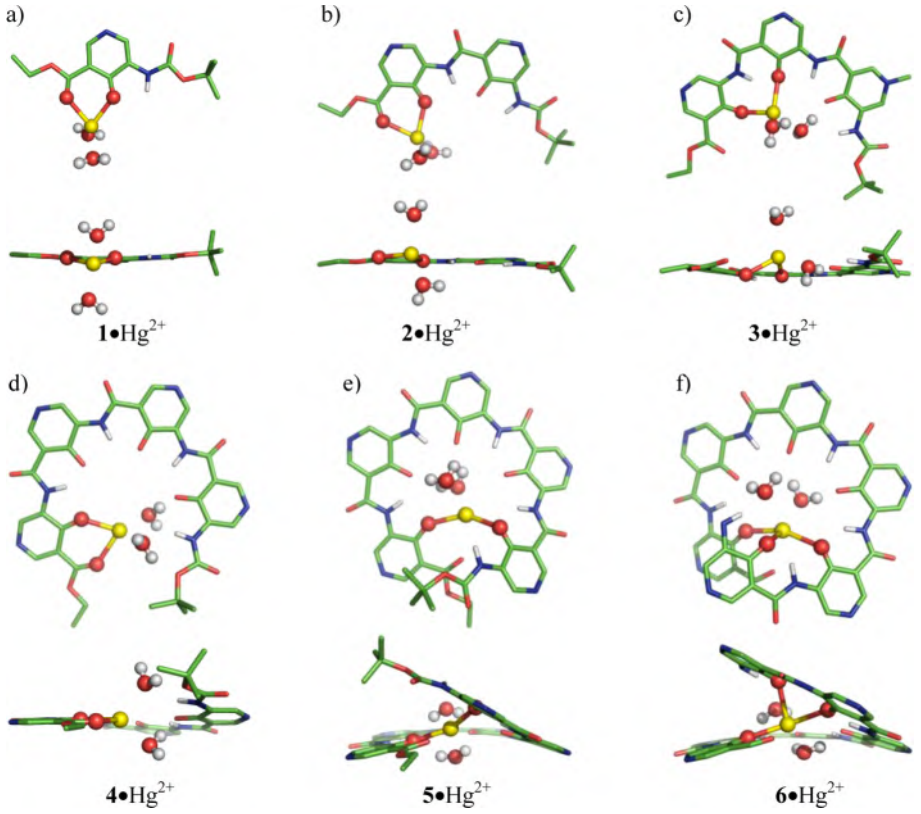

Figure 4. Computationally determined structures at the B3LYP/6-31G(d,p) level for the most stable water-containing complexes $[Hg^{2+}(n)(H_2O)_2]$ (n = **1**−**6**) using chloroform as the explicit solvent. Interior O atoms from the aromatic backbones involved in the direct bonding to Hg^{2+} ions are highlighted as red balls. In other words, these O atoms are within 2.6 Å distance from Hg^{2+} ions. All water molecules also form strong coordination bonds with the bound Hg^{2+} ion, and H-bonds with the backbones. For clarity of view, exterior side chains and nonamide H atoms in pyridone units were all removed; in panel f, the end Boc and OEt groups were also removed. In these computed structures, Hg^{2+} ions are 4-coordinate in **1**−**5** and five-coordinate in **6**.

with Hg^{2+} ions at 500, 50 and 20 ppb, i.e., at 2.5, 0.25 and 0.10 μM, respectively. The corresponding molar ratios involving total competing metal ions (Na^+, K^+, Ca^{2+} and Mg^{2+} ions) at 6.946 mM vs Hg^{2+} at 2.5, 0.25 and 0.10 μM are 2778:1, 27780:1 and 69460:1, respectively. Despite such excessive amounts of competing metal ions present in solution, mercury extraction efficiencies using **4** at a constant [**4**]:[Hg^{2+}] molar ratio of 5:1 still could reach 57, 50 and 42%, respectively.

The above data suggest that high-capacity extraction of Hg^{2+} ions by **4** is well-maintained at concentration ranges of 5−2000 ppb in pure water and of 10−2000 ppb in artificial groundwater. In other words, the concentration of a solution containing Hg^{2+} at 20 ppm (or 0.1 mM) can be lowered to 4 ppb via two successive biphasic extractions using **4** at 0.2 and 0.05 mM in $CHCl_3$ of equal volumes, respectively. The overall consumption of **4** is therefore 0.25 mM per 0.1 mM of Hg^{2+} in equal volume or 14.4 mg of **4** per 1 mg of Hg^{2+} ions. For artificial groundwater, the minimum consumption of **4** to reduce Hg^{2+} from 500 ppb (2.5 μM) to below 10 ppb roughly is 9:1 in [**4**]:[Hg^{2+}] molar ratio or 52:1 in **4**:Hg^{2+} mass ratio.

Computational Insights into Structures of Hydrated Hg^{2+}-Containing Complexes. Unlike most of other hydrated metal nitrates that contain six or more water molecules in their inner coordination sphere, Hg^{2+} ions are coordinated to only four water molecules in their most common form. This, in part, might explain the remarkably high selectivity in binding Hg^{2+} ions by **1**−**6** as formation of mercury complexes requires less water molecules to be removed. What still puzzles us is how **3**−**6**, having a cavity of ∼1.6 Å in radius, can efficiently bind Hg^{2+} ions with an ionic radius of 1.02 Å. To help shed some light onto the possibly formed structures, calculations at the B3LYP/6-31G(d,p) level using chloroform as the explicit solvent were performed to yield the most stable hydrated Hg^{2+}-containing complexes for **1**−**6** (Figure 4) with the structures and relative energies for other alternative isomeric complexes listed in Figures S1−S5.[12]

In all complexes formed by **1**−**6**, the first pyridone unit from the ester end seems to be instrumental in forming good to tight complexes with Hg^{2+} ions, and the outward-pointing bulky *tert*-butyl groups appears to exert little influence on ion-binding. The carbonyl O atom from the end ester group also plays a decisive role in complex formation for short foldarands **1**, **2** and **4**, but for helically folded **5** and **6**, the additional bonding contributions to forming a tight complex with Hg^{2+} ions arise from one or two more pyridone units. Interestingly, the central pyridone unit makes good contributions to the complex formation only for **3**, presumably as a result of unfavored repulsion between the amide proton, which is located between two adjacent Hg^{2+}-binding pyridone units, and the Hg^{2+} ion (Figure 4c). This significant repulsion actually makes the Hg^{2+} ion deviate substantially from the plane defined by the binding O atoms. In addition to their direct bonding to the Hg^{2+} ion, two water molecules also serve as the bridge atoms to fill in the excessive cavity space unoccupied by the Hg^{2+} ion. Starting from trimer, these two water molecules further help to stabilize the complexes by forming 2, 3, 4 and 5 H-bonds with the

DOI: 10.1021/jacs.6b13342
J. Am. Chem. Soc. 2017, 139, 5387−5396

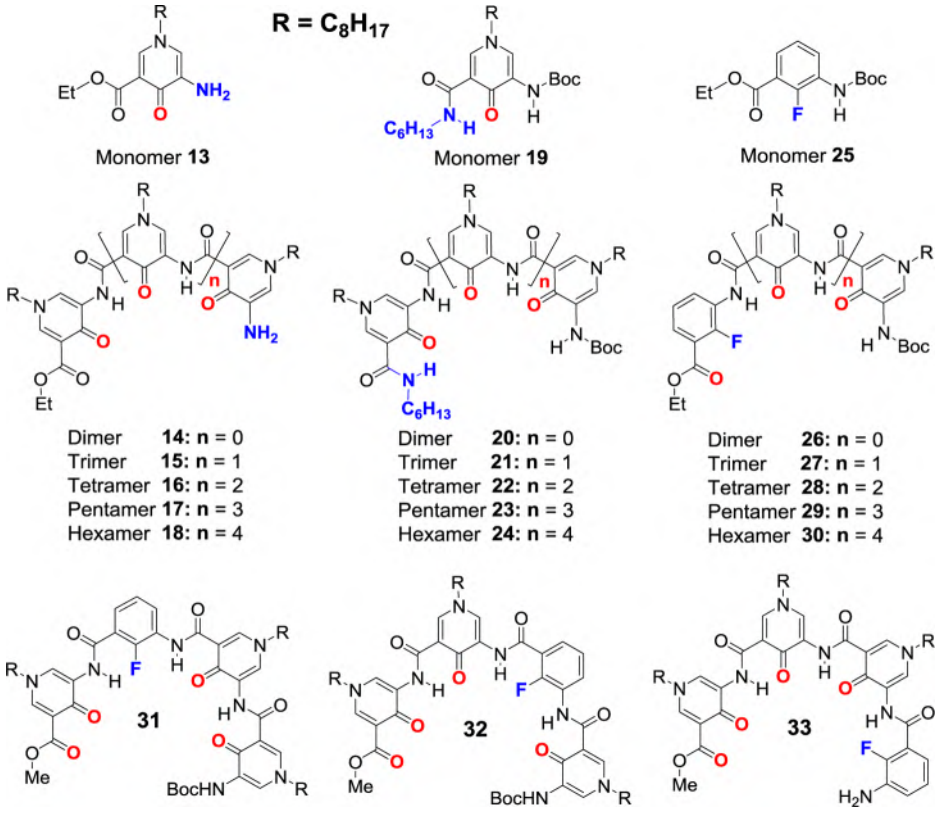

Figure 5. Structures of four series of foldarands **13**−**33** varied from **1**−**6** at selected positions (highlighted in blue) for deducing the preferential binding sites recognized by Hg^{2+} ions and for validating computational findings.

aromatic backbones in **3**−**6**, respectively. Except for complex **1**·Hg^{2+}, all other complexes could be additionally stabilized by distant electrostatic forces arising from adjacent nonbonding pyridone units and ester carbonyl O atoms, enabling mercury-binding capacity to increase in the order of **1** < **2** < **3** < **4** ≈ **5** ≈ **6**. Lastly, from the computed structures, it can be seen that the presence of intramolecular H-bond directs the bulky *tert*-butyl group away from both the cavity center and the bound Hg^{2+} ion and two water molecules in all complexes (Figure 4). As such, it is expected that these bulky groups have limited influence on the Hg^{2+}-binding capacity of foldarands **1**−**6** toward metal ions.

Although it remains difficult to elucidate computationally the binding selectivity origin at the structural level, speculatively, water molecules and associated hydration energies may play an important role in the observed selectivities. From the computed structure involving **3**−**6**, a sufficient space clearly exists for two but only two water molecules to stay comfortably within the cavity, which account for half of total water molecules around the Hg^{2+} ion and make dehydration a less painful process for recognition of Hg^{2+} ion. In contrast, for Na^+, K^+ and Ca^{2+} ions that carry at least six water molecules, the inner cavity in **3**−**6**, however, could provide an additional space for accommodating no more than three water molecules in **3** and likely only two water molecules in **4**−**6**. The corresponding dehydration processes therefore cannot take place readily for Na^+, K^+ and Ca^{2+} ions when compared to Hg^{2+} ions.

Experimental Evidence to Support Computational Findings. On the basis of computed structures, four series of oligomers, i.e., **13**−**18**, **19**−**24**, **25**−**30** and **28**/**31**−**33** (Figure 5), which were varied from **1**−**6** at selected pin-pointed positions, were prepared to assess experimentally the binding preferences on binding sites by Hg^{2+} ions for comparison with those computationally elucidated binding features. For all foldarands **13**−**33**, biphasic ion extractions were carried out using host at 0.9 mM against a total of 18 metal ions at [total of metal ions] = 1.8 mM to elucidate selectivity and total capacity in ion binding (Table S2), and using host at 2.5 μM against only Hg^{2+} ion at the same concentration of 2.5 μM to determine the ion binding capacity toward Hg^{2+} ions (Table 2).

Table 2. Extraction Efficiencies (%) of Hg^{2+} Ions at 2.5 μM by Foldarands 1−6 and 13−33 at 2.5 μM[a]

1	20	**13**	13	**19**	3	**25**	–[b]	**31**	53
2	28	**14**	23	**20**	5	**26**	–[b]	**32**	52
3	49	**15**	40	**21**	21	**27**	5	**33**	45
4	64	**16**	57	**22**	33	**28**	13		
5	66	**17**	56	**23**	47	**29**	25		
6	62	**18**	56	**24**	45	**30**	20		

[a]Extractions were carried out in a biphasic system using equal volumes of H_2O containing Hg^{2+} ions at 2.5 μM and $CHCl_3$ containing host at 2.5 μM at 25 °C, and extractions were determined by using ICP-MS. All reported data are averaged values over six runs with relative errors within 1%. [b]No extraction.

We first looked into the effect of removing the end bulky *tert*-butyl groups in **1**−**6** on ion binding capacity and selectivity of resultant amine-containing foldarands **13**−**18**. Comparison of extraction data at [host] = 0.9 mM and [total metal ions] = 1.8 mM between Boc-containing **1**−**6** (Table S1) and amine-containing **13**−**18** (Table S2) reveals insignificant difference in both ion selectivity and total ion binding capacity. The main difference between the two groups of ligands lies in the

DOI: 10.1021/jacs.6b13342
J. Am. Chem. Soc. 2017, 139, 5387−5396

extraction of Ag^+ ions. That is, Ag^+ ions become significantly more extractable by **13**−**18** than by **1**−**6**, and to such an extent that pentamer **17** and hexamer **18** display equal ability to extract both Hg^{2+} and Ag^+ ions, and that extractions of Hg^{2+} ions by **13**−**18** decrease by 11−17%. However, in the absence of all other metal ions, individual extractions against only Hg^{2+} ions at 2.5 μM using host at 2.5 μM produce minor differences in Hg^{2+} recognition between **1**−**6** and **13**−**18** (Table 2). These results, which are in line with the above computational findings, confirm insignificant impacts bulky *tert*-butyl groups have in Hg^{2+} recognition.

The contribution of ester carbonyl O atom toward ion recognition was then investigated. Although biphasic extraction in the presence of 18 metal ions also establishes the highly selective nature of **19**−**22** in recognizing Hg^{2+} ion (Table S2), the individual extractions using only Hg^{2+} ions give rise to more insights into the binding features at the structural level. At [host] = 2.5 μM and with a [host]:[Hg^{2+}] molar ratio of 1:1, Hg^{2+} extraction percentages drop by 85, 82, 57, 58, 29 and 27% for **19**−**24** when compared to **1**−**6** (Table 2), respectively. These data are consistent with the pivotal stabilization of complexes via Hg^{2+}−O coordination bonds mediated by the ester O atoms for **1**, **2** and **4** (Figure 4a,b,d), and simple replacement of the ester group with an amide group almost completely aborts the Hg^{2+}-binding ability of **19** and **20** with **22** only able to recover partially its binding ability via both alternative binding sites and electrostatically attractive forces arising from adjacent pyridone O atoms. These data are also consistent with minor stabilization of complexes provided by the ester O atoms in **5** and **6** (Figure 4e,f). That is, introduction of an amide group as in **23** and **24** most likely exerts little impact on their Hg^{2+}-binding ability. Instead, the observed reductions by 19 and 17% in extraction should result from the strong repulsive interactions between the introduced amide proton and the bound Hg^{2+} ion in proximity. For the same reason, such repulsive forces lead to a significant reduction of 28% in Hg^{2+} extraction for **21**, which, unlike **23** and **24** that carry three distant O atoms, has the luxury of only one distant O atom for helping stabilize the bound Hg^{2+} ion.

Because the first pyridone unit from the ester end was computationally determined to be involved in binding Hg^{2+} ions in all complexes formed by **1**−**6**, we also evaluated the effect of substituting the first pyridone unit with a fluorinated build block not only because the fluorobenzene unit is geometrically compatible with the curving backbone[4k,13] but also because the covalently linked fluorine atom has been shown to be a poor donor atom for metal ions.[4k] As shown in Table 2, the ability of the singly substituted **25**−**30** to extract Hg^{2+} ions decreases very dramatically with no extractions by **25** and **26**, and relative reductions in Hg^{2+} extraction by 90% for **27**, 80% for **28**, 62% for **29** and 68% for **30** when normalized based on **1**−**6** (Table 2). As revealed computationally, these deleterious effects, arising from just a single fluorobenzene unit, unambiguously confirm the involvement and critical role of the first pyridone unit in binding and stabilizing the bound Hg^{2+} ion in all complexes.

Further, given that tetramer **4** exhibits the highest binding capacity and selectivity among **1**−**6**, we naturally became intrigued to determine the exact binding sites preferred by Hg^{2+} ions. For this purpose, three more variants **31**−**33**, together with **28**, were made. Compared to **4** able to remove 64% Hg^{2+} ions, replacements of one pyridone unit at various locations with a fluorobenzene motif result in differential mercury extractions of 13% for **28**, 53% for **31**, 52% for **32** and 45% for **33**. The largest reduction in Hg^{2+} extraction observed for **28** and much smaller reductions for **31**−**33** are fully consistent with the structural features of the computationally determined most stable **4**−Hg^{2+} complex (Figure 4d and Figure S3), revealing participation of the first pyridone unit and the only unit in forming two stabilizing coordination bonds with the Hg^{2+} ion and additional stabilization of the complex by the three distant nonbonding pyridone O atoms at positions 2−4 via electrostatic interactions. From the computed structure (Figure 4d), one of the two water molecules forms a strong H-bond with the pyridone O atom at position 4. Replacing the pyridone at position 4 with a fluorobenzene unit must have weakened the corresponding H-bond upon a change in H-bond acceptor from O- to F atom. This weakened H-bond could account for the weakened ability of **33** to extract Hg^{2+} ions relative to **31** and **32** (Table 2).

Lastly, it might be worth pointing out that some minor variations in structure do allow for fine-tuning the ion-binding selectivity from Hg^{2+} to Cs^+ ion for **23**, **24** and **30** and to K^+ ion for **27** (Table S2), suggesting a possibility of modulating the ion-binding selectivity further using fluorobenzene, methoxy, anionic or other types of building blocks that are geometrically compatible with the pyridone-based folding backbones of **1**−**6**[4f,k] or by introducing highly curved pyridine units.[2l,5o]

CONCLUSION

In summary, we have successfully established here a foldamer-based approach toward construction of a unique class of ion-binding foldarands with a rigid conformation conducive to cation recognition. Their intrinsic folding into crescent-shaped planar or helically folded conformations not only present a cation with a convergently aligned array of electron-rich O atoms but also creates a suitable and rigid cavity for comfortably accommodating a partially hydrated metal ion. These features enable the foldarands studied herein to achieve both high binding affinity and high selectivity in recognizing Hg^{2+} ion in the presence of 22 other metal ions with performance superior over different classes of ligands, including crown ethers, thio-crown ethers and valinomycin. As elucidated computationally and corroborated by systematic structural investigations, the stabilization of these Hg^{2+}-containing complexes involves critical contributions from the first pyridone motif at the ester end for all foldarand molecules of varying lengths studied herein, with additional assistances from the ester carbonyl O atom for monomer, dimer and tetramer and from other pyridone O atoms for trimer, pentamer and hexamer. With the use of tetrameric foldarand **4**, level of Hg^{2+} ions can be effectively maintained below 10 ppb in artificial groundwater and below 5 ppb in pure water using a binary solvent extraction method, which is widely recognized as a viable and energy-saving technique suitable for removal or separation of toxic metal ions. As an alternative to smelly sulfur-containing molecules, these mercury-scavenging foldarands might find some practical uses in environmental remediation of mercury contamination. Given their modularly tunable backbones, further refinement in ion-binding selectivity is possible upon incorporation of geometrically compatible building blocks containing inward-pointing functional groups of various types.[2l,4f,k,5o]

DOI: 10.1021/jacs.6b13342
J. Am. Chem. Soc. 2017, 139, 5387−5396

■ ASSOCIATED CONTENT

Supporting Information

The Supporting Information is available free of charge on the ACS Publications website at DOI: 10.1021/jacs.6b13342.

Synthetic procedures for **6** and **12**−**33** as well as a full set of characterization data including ^{1}H NMR, ^{13}C NMR, (HR)MS, ICP data for **1**−**33** and computational details (PDF)

X-ray crystal file/data sheet for **12** (CIF)

■ AUTHOR INFORMATION

Corresponding Author

*hqzeng@ibn.a-star.edu.sg

ORCID

Huaqiang Zeng: 0000-0002-8246-2000

Notes

The authors declare no competing financial interest.

■ ACKNOWLEDGMENTS

This work was supported by the Institute of Bioengineering and Nanotechnology (Biomedical Research Council, Agency for Science, Technology and Research, Singapore) and the Singapore National Research Foundation under its Environment and Water Research Programme and administered by PUB.

■ REFERENCES

(1) (a) Gellman, S. H. *Acc. Chem. Res.* **1998**, *31*, 173. (b) Hill, D. J.; Mio, M. J.; Prince, R. B.; Hughes, T. S.; Moore, J. S. *Chem. Rev.* **2001**, *101*, 3893. (c) Cheng, R. P. *Curr. Opin. Struct. Biol.* **2004**, *14*, 512. (d) Goodman, C. M.; Choi, S.; Shandler, S.; DeGrado, W. F. *Nat. Chem. Biol.* **2007**, *3*, 252. (e) Gong, B. *Acc. Chem. Res.* **2008**, *41*, 1376. (f) Horne, W. S.; Gellman, S. H. *Acc. Chem. Res.* **2008**, *41*, 1399. (g) Li, Z. T.; Hou, J. L.; Li, C. *Acc. Chem. Res.* **2008**, *41*, 1343. (h) Saraogi, I.; Hamilton, A. D. *Chem. Soc. Rev.* **2009**, *38*, 1726. (i) Hua, Y.; Flood, A. H. *Chem. Soc. Rev.* **2010**, *39*, 1262. (j) Juwarker, H.; Jeong, K.-S. *Chem. Soc. Rev.* **2010**, *39*, 3664. (k) Guichard, G.; Huc, I. *Chem. Commun.* **2011**, *47*, 5933. (l) Zhang, D.-W.; Zhao, X.; Hou, J.-L.; Li, Z.-T. *Chem. Rev.* **2012**, *112*, 5271. (m) Yamato, K.; Kline, M.; Gong, B. *Chem. Commun.* **2012**, *48*, 12142. (n) Ong, W. Q.; Zeng, H. Q. *J. Inclusion Phenom. Mol. Recognit. Chem.* **2013**, *76*, 1. (o) Fu, H. L.; Liu, Y.; Zeng, H. Q. *Chem. Commun.* **2013**, *49*, 4127. (p) Huo, Y. P.; Zeng, H. Q. *Acc. Chem. Res.* **2016**, *49*, 922.

(2) (a) Hou, J. L.; Shao, X. B.; Chen, G. J.; Zhou, Y. X.; Jiang, X. K.; Li, Z. T. *J. Am. Chem. Soc.* **2004**, *126*, 12386. (b) Inouye, M.; Waki, M.; Abe, H. *J. Am. Chem. Soc.* **2004**, *126*, 2022. (c) Waki, M.; Abe, H.; Inouye, M. *Angew. Chem., Int. Ed.* **2007**, *46*, 3059. (d) Garric, J.; Leger, J.-M.; Huc, I. *Angew. Chem., Int. Ed.* **2005**, *44*, 1954. (e) Ong, W. Q.; Zhao, H. Q.; Fang, X.; Woen, S.; Zhou, F.; Yap, W. L.; Su, H. B.; Li, S. F. Y.; Zeng, H. Q. *Org. Lett.* **2011**, *13*, 3194. (f) Zhao, H. Q.; Ong, W. Q.; Fang, X.; Zhou, F.; Hii, M. N.; Li, S. F. Y.; Su, H. B.; Zeng, H. Q. *Org. Biomol. Chem.* **2012**, *10*, 1172. (g) Ma, W. L.; Wang, C. Q.; Li, J. T.; Zhang, K.; Lu, Y.-J.; Huo, Y. P.; Zeng, H. Q. *Org. Biomol. Chem.* **2015**, *13*, 10613. (h) Jeon, H.-G.; Jung, J. Y.; Kang, P.; Choi, M.-G.; Jeong, K.-S. *J. Am. Chem. Soc.* **2016**, *138*, 92. (i) Tanatani, A.; Mio, M. J.; Moore, J. S. *J. Am. Chem. Soc.* **2001**, *123*, 1792. (j) Nishinaga, T.; Tanatani, A.; Oh, K.; Moore, J. S. *J. Am. Chem. Soc.* **2002**, *124*, 5934. (k) Gan, Q.; Ferrand, Y.; Bao, C.; Kauffmann, B.; Grélard, A.; Jiang, H.; Huc, I. *Science* **2011**, *331*, 1172. (l) Zhao, H. Q.; Ong, W. Q.; Zhou, F.; Fang, X.; Chen, X. Y.; Li, S. F. Y.; Su, H. B.; Cho, N.-J.; Zeng, H. Q. *Chem. Sci.* **2012**, *3*, 2042. (m) Ong, W. Q.; Zhao, H. Q.; Sun, C.; Wu, J. E.; Wong, Z. C.; Li, S. F. Y.; Hong, Y. H.; Zeng, H. Q. *Chem. Commun.* **2012**, *48*, 6343. (n) Sun, C.; Ren, C. L.; Wei, Y. C.; Qin, B.; Zeng, H. Q. *Chem. Commun.* **2013**, *49*, 5307. (o) Sun, C.; Liu, Y.; Liu, J. Q.; Lu, Y.-J.; Yu, L.; Zhang, K.; Zeng, H. Q. *J. Org. Chem.* **2014**, *79*, 2963. (p) Chandramouli, N.; Ferrand, Y.; Lautrette, G.; Kauffmann, B.; Mackereth, C. D.; Laguerre, M.; Dubreuil, D.; Huc, I. *Nat. Chem.* **2015**, *7*, 334.

(3) (a) Lehn, J.-M.; Rigault, A.; Siegel, J.; Harrowfield, J.; Chevrier, B.; Moras, D. *Proc. Natl. Acad. Sci. U. S. A.* **1987**, *84*, 2565. (b) Bernardinelli, G.; Piguet, C.; Williams, A. F. *Angew. Chem., Int. Ed. Engl.* **1992**, *31*, 1622. (c) Constable, E. C. *Tetrahedron* **1992**, *48*, 10013. (d) Bell, T. W.; Jousselin, H. *Nature* **1994**, *367*, 441. (e) Albrecht, M. *Chem. Rev.* **2001**, *101*, 3457. (f) Stadler, A.-M.; Lehn, J.-M. P. *J. Am. Chem. Soc.* **2014**, *136*, 3400−3409. (g) Prince, R. B.; Okada, T.; Moore, J. S. *Angew. Chem., Int. Ed.* **1999**, *38*, 233. (h) Mizutani, T.; Yagi, S.; Morinaga, T.; Nomura, T.; Takagishi, T.; Kitagawa, S.; Ogoshi, H. *J. Am. Chem. Soc.* **1999**, *121*, 754. (i) Li, C.; Ren, S.-F.; Hou, J.-L.; Yi, H.-P.; Zhu, S.-Z.; Jiang, X.-K.; Li, Z.-T. *Angew. Chem., Int. Ed.* **2005**, *44*, 5725.

(4) (a) Sanford, A. R.; Yuan, L. H.; Feng, W.; Yamato, K.; Flowers, R. A.; Gong, B. *Chem. Commun.* **2005**, 4720. (b) Zhang, F.; Bai, S.; Yap, G. P. A.; Tarwade, V.; Fox, J. M. *J. Am. Chem. Soc.* **2005**, *127*, 10590. (c) Dong, Z.; Karpowicz, R. J.; Bai, S.; Yap, G. P. A.; Fox, J. M. *J. Am. Chem. Soc.* **2006**, *128*, 14242. (d) Zhao, Y.; Zhong, Z. Q. *J. Am. Chem. Soc.* **2006**, *128*, 9988. (e) Li, Y.; Flood, A. H. *J. Am. Chem. Soc.* **2008**, *130*, 12111. (f) Qin, B.; Ren, C. L.; Ye, R. J.; Sun, C.; Chiad, K.; Chen, X. Y.; Li, Z.; Xue, F.; Su, H. B.; Chass, G. A.; Zeng, H. Q. *J. Am. Chem. Soc.* **2010**, *132*, 9564. (g) Ren, C. L.; Maurizot, V.; Zhao, H. Q.; Shen, J.; Zhou, F.; Ong, W. Q.; Du, Z. Y.; Zhang, K.; Su, H. B.; Zeng, H. Q. *J. Am. Chem. Soc.* **2011**, *133*, 13930. (h) Suk, J.-M.; Naidu, V. R.; Liu, X.; Lah, M. S.; Jeong, K.-S. *J. Am. Chem. Soc.* **2011**, *133*, 13938. (i) Tashiro, S.; Matsuoka, K.; Minoda, A.; Shionoya, M. *Angew. Chem., Int. Ed.* **2012**, *51*, 13123. (j) Shen, J.; Ma, W. L.; Yu, L.; Li, J.-B.; Tao, H.-C.; Zhang, K.; Zeng, H. Q. *Chem. Commun.* **2014**, *50*, 12730. (k) Liu, Y.; Shen, J.; Sun, C.; Zeng, H. Q.; Ren, C. *J. Am. Chem. Soc.* **2015**, *137*, 12055. (l) Ren, C. L.; Shen, J.; Zeng, H. Q. *Org. Lett.* **2015**, *17*, 5946. (m) Shen, J.; Ren, C. L.; Zeng, H. Q. *Chem. Commun.* **2016**, *52*, 10361.

(5) (a) Shirude, P. S.; Gillies, E. R.; Ladame, S.; Godde, F.; Shin-Ya, K.; Huc, I.; Balasubramanian, S. *J. Am. Chem. Soc.* **2007**, *129*, 11890. (b) Buratto, J.; Colombo, C.; Stupfel, M.; Dawson, S. J.; Dolain, C.; Langlois d'Estaintot, B.; Fischer, L.; Granier, T.; Laguerre, M.; Gallois, B.; Huc, I. *Angew. Chem.* **2014**, *126*, 902. (c) Cai, W.; Wang, G. T.; Xu, Y. X.; Jiang, X. K.; Li, Z. T. *J. Am. Chem. Soc.* **2008**, *130*, 6936. (d) Ren, C. L.; Xu, S. Y.; Xu, J.; Chen, H. Y.; Zeng, H. Q. *Org. Lett.* **2011**, *13*, 3840. (e) He, Y. Z.; Xu, M.; Gao, R. Z.; Li, X. W.; Li, F. X.; Wu, X. D.; Xu, D. G.; Zeng, H. Q.; Yuan, L. H. *Angew. Chem., Int. Ed.* **2014**, *53*, 11834. (f) Li, X. W.; Li, B.; Chen, L.; Hu, J. C.; Wen, C.; Zheng, Q. D.; Wu, L. X.; Zeng, H. Q.; Gong, B.; Yuan, L. H. *Angew. Chem., Int. Ed.* **2015**, *54*, 11147. (g) Hooley, R. J.; Rebek, J., Jr *Chem. Biol.* **2009**, *16*, 255. (h) Muller, M. M.; Windsor, M. A.; Pomerantz, W. C.; Gellman, S. H.; Hilvert, D. *Angew. Chem., Int. Ed.* **2009**, *48*, 922. (i) Srinivas, K.; Kauffmann, B.; Dolain, C.; Leger, J. M.; Ghosez, L.; Huc, I. *J. Am. Chem. Soc.* **2008**, *130*, 13210. (j) Zhao, H. Q.; Shen, J.; Guo, J. J.; Ye, R. J.; Zeng, H. Q. *Chem. Commun.* **2013**, *49*, 2323. (k) Smaldone, R. A.; Moore, J. S. *J. Am. Chem. Soc.* **2007**, *129*, 5444. (l) Hu, H.-Y.; Xiang, J.-F.; Cao, J.; Chen, C.-F. *Org. Lett.* **2008**, *10*, 5035. (m) Qin, B.; Jiang, L. Y.; Shen, S.; Sun, C.; Yuan, W. X.; Li, S. F. Y.; Zeng, H. Q. *Org. Lett.* **2011**, *13*, 6212. (n) Du, Z. Y.; Qin, B.; Sun, C.; Liu, Y.; Zheng, X.; Zhang, K.; Conney, A. H.; Zeng, H. Q. *Org. Biomol. Chem.* **2012**, *10*, 4164. (o) Zhao, H. Q.; Sheng, S.; Hong, Y. H.; Zeng, H. Q. *J. Am. Chem. Soc.* **2014**, *136*, 14270. (p) Helsel, A. J.; Brown, A. L.; Yamato, K.; Feng, W.; Yuan, L. H.; Clements, A. J.; Harding, S. V.; Szabo, G.; Shao, Z. F.; Gong, B. *J. Am. Chem. Soc.* **2008**, *130*, 15784. (q) Zhao, Y.; Cho, H.; Widanapathirana, L.; Zhang, S. *Acc. Chem. Res.* **2013**, *46*, 2763. (r) Xin, P.; Zhu, P.; Su, P.; Hou, J.-L.; Li, Z.-T. *J. Am. Chem. Soc.* **2014**, *136*, 13078. (s) Wei, X.; Zhang, G.; Shen, Y.; Zhong, Y.; Liu, R.; Yang, N.; Al-mkhaizim, F. Y.; Kline, M. A.; He, L.; Li, M.; Lu, Z.-L.; Shao, Z.; Gong, B. *J. Am. Chem. Soc.* **2016**, *138*, 2749. (t) Lang, C.; Li, W.; Dong, Z.; Zhang, X.; Yang, F.; Yang, B.; Deng, X.; Zhang, C.; Xu, J.; Liu, J. *Angew. Chem., Int. Ed.* **2016**, *55*, 9723. (u) Li, X.; Markandeya, N.; Jonusauskas, G.; McClenaghan, N. D.; Maurizot, V.; Denisov, S. A.; Huc, I. *J. Am. Chem. Soc.* **2016**, *138*, 13568.

DOI: 10.1021/jacs.6b13342
J. Am. Chem. Soc. 2017, 139, 5387−5396

(6) (a) Pedersen, C. J. *J. Am. Chem. Soc.* **1967**, *89*, 2415. (b) Pedersen, C. J. *J. Am. Chem. Soc.* **1967**, *89*, 7017. (c) Dietrich, B.; Lehn, J.-M.; Sauvage, J.-P. *Tetrahedron Lett.* **1969**, *10*, 2885. (d) Dietrich, B.; Lehn, J.-M.; Sauvage, J.-P. *Tetrahedron Lett.* **1969**, *10*, 2889. (e) Kyba, E. P.; Siegel, M. G.; Sousa, L. R.; Sogah, G. D. Y.; Cram, D. J. *J. Am. Chem. Soc.* **1973**, *95*, 2691. (f) Helgeson, R. C.; Koga, K.; Timko, J. M.; Cram, D. J. *J. Am. Chem. Soc.* **1973**, *95*, 3021. (g) Bell, T. W.; Cragg, P. J.; Drew, M. G. B.; Firestone, A.; Kwok, D. I. A. *Angew. Chem., Int. Ed. Engl.* **1992**, *31*, 345. (h) Bell, T. W.; Cragg, P. J.; Drew, M. G. B.; Firestone, A.; Kwok, D. I. A. *Angew. Chem., Int. Ed. Engl.* **1992**, *31*, 348.

(7) Qi, T.; Maurizot, V.; Noguchi, H.; Charoenraks, T.; Kauffmann, B.; Takafuji, M.; Ihara, H.; Huc, I. *Chem. Commun.* **2012**, *48*, 6337.

(8) (a) Kanamori, D.; Okamura, T. A.; Yamamoto, H.; Ueyama, N. *Angew. Chem., Int. Ed.* **2005**, *44*, 969. (b) Zhu, J.; Parra, R. D.; Zeng, H. Q.; Skrzypczak-Jankun, E.; Zeng, X. C.; Gong, B. *J. Am. Chem. Soc.* **2000**, *122*, 4219. (c) Hou, J.-L.; Yi, H.-P.; Shao, X.-B.; Li, C.; Wu, Z.-Q.; Jiang, X.-K.; Wu, L.-Z.; Tung, C.-H.; Li, Z.-T. *Angew. Chem., Int. Ed.* **2006**, *45*, 796. (d) Yan, Y.; Qin, B.; Shu, Y. Y.; Chen, X. Y.; Yip, Y. K.; Zhang, D. W.; Su, H. B.; Zeng, H. Q. *Org. Lett.* **2009**, *11*, 1201. (e) Yan, Y.; Qin, B.; Ren, C. L.; Chen, X. Y.; Yip, Y. K.; Ye, R. J.; Zhang, D. W.; Su, H. B.; Zeng, H. Q. *J. Am. Chem. Soc.* **2010**, *132*, 5869.

(9) (a) Qin, B.; Chen, X. Y.; Fang, X.; Shu, Y. Y.; Yip, Y. K.; Yan, Y.; Pan, S. Y.; Ong, W. Q.; Ren, C. L.; Su, H. B.; Zeng, H. Q. *Org. Lett.* **2008**, *10*, 5127. (b) Ong, W. Q.; Zhao, H. Q.; Du, Z. Y.; Yeh, J. Z. Y.; Ren, C. L.; Tan, L. Z. W.; Zhang, K.; Zeng, H. Q. *Chem. Commun.* **2011**, *47*, 6416.

(10) Ritter, J. A.; Bibler, J. P. *Water Sci. Technol.* **1992**, *25*, 165.

(11) (a) Miretzky, P.; Cirelli, A. F. *J. Hazard. Mater.* **2009**, *167*, 10. (b) Wang, J.; Feng, X.; Anderson, C. W. N.; Xing, Y.; Shang, L. *J. Hazard. Mater.* **2012**, *221−222*, 1. (c) Blue, L. Y.; Van Aelstyn, M. A.; Matlock, M.; Atwood, D. A. *Water Res.* **2008**, *42*, 2025. (d) Byrne, H. E.; Mazyck, D. W. *J. Hazard. Mater.* **2009**, *170*, 915. (e) Parham, H.; Zargar, B.; Shiralipour, R. *J. Hazard. Mater.* **2012**, *205−206*, 94. (f) Lu, X.; Huangfu, X.; Ma, J. *J. Hazard. Mater.* **2014**, *280*, 71.

(12) Although multistranded helicates cannot be completely ruled out, the chance of forming such structures is quite slim. One main reason is that the ligands studied in our current work do not adopt an extended structure. Instead, they all take a crescent-shaped or helically folded conformation containing a near-planar cavity that readily provides an ample space for accommodating a partially hydrated Hg^{2+} ion, which could be additionally stabilized by some adjacent electron-rich O atoms within the same molecule. In fact, we have done the calculations for the dimeric structure formed from one Hg^{2+} ion and two molecules of either monomer **1** or dimer **2** (e.g., $[Hg^{2+}(\mathbf{1})_2]$ and $[Hg^{2+}(\mathbf{2})_2]$), and compare their binding energies with their corresponding partially hydrated Hg^{2+}-containing complexes (e.g., $[Hg^{2+}(\mathbf{1})(H_2O)_2]$ and $[Hg^{2+}(\mathbf{2})(H_2O)_2]$). We found that dimeric structures are less stable than partially hydrated monomeric structures by 5.5 and 7.4 kcal/mol, respectively. Further considering (1) very rigid and crowded structure seen in trimer, tetramer, petnamer and hexamer and (2) a small radius of 1.16 Å for the Hg^{2+} ion, forming dimeric or oligomeric helicates to wrap around the Hg^{2+} ion likely is not an energetically favored process.

(13) Ren, C. L.; Zhou, F.; Qin, B.; Ye, R. J.; Shen, S.; Su, H. B.; Zeng, H. Q. *Angew. Chem., Int. Ed.* **2011**, *50*, 10612.

■ NOTE ADDED AFTER ASAP PUBLICATION

A revised version of the Supporting Information was uploaded on March 1, 2017 after the initial publication on February 9, 2017. The scheme outlining compounds **1**−**11** was added on April 5, 2017.

DOI: 10.1021/jacs.6b13342
J. Am. Chem. Soc. 2017, 139, 5387−5396